Research Article

Received: 3 December 2023 Revised: 25 March 2024 Published online in Wiley Online Library:

(wileyonlinelibrary.com) DOI 10.1002/jctb.7681

Green synthesis of silver nanoparticles using leaf extract of *Woodfordia fruticosa (L.)* for potential therapeutic application

Debasmita Dubey,[a] Rajesh Kumar Meher,[b] Biswaranjan Pradhan,[c] Sadhni Induar,[d] Biswakanth Kar,[e] Pradeep Kumar Naik[b] and Bikash Chandra Behera[f*]

Abstract

BACKGROUND: *Woodfordia fruticosa* is a well-known medicinal plant traditionally used for various treatment methods. Green synthesis of silver nanocomposite with *woodfordia* flower extract is well-investigated. However, the therapeutic potential of *Woodfordia fruticosa* leaf extract silver nanoparticles against various diseases has yet to be investigated.

RESULTS: Silver nanoparticles synthesized from *Woodfordia fruticosa* leaf extract (Wf-AgNPs) showed UV spectral peaks at 450 nm. Transmission electron microscope (TEM) images, ranging from 20 to 50 nm, confirm the nanosynthesis. The average particle size of 39.63 nm with a zeta potential distribution value 17.0 was observed. Fourier transform infrared peaks ranging from 2942to 669 cm^{-1} confirm the amines, amides, carboxylic, aldehyde, alkane, phenolic and aliphatic bromo compounds involved in the synthesis of AgNPs. Wf-AgNPs showed higher antioxidant activity compared to the ascorbic acid and BHT. The phenolic and flavonoid content was 141.66 $\pm$ 8.50 mg GAE/100 g dry weight and 191.66 $\pm$ 5.6 mg quercetin equivalent/100 g dry weight, respectively. Wf-AgNPs showed a strong inverse relationship between the dose and viability of the cancer cells. The antibacterial properties of Wf-AgNPs were confirmed through the bacteria's SEM images. Increased wound healing potential, re-epithelization and elevation of the tensile strength of the infected skin tissue were observed after applying synthesized Wf-AgNPs.

CONCLUSION: Various phytochemicals in the synthesized nanoparticles confer antimicrobial, antioxidant, anticancer and wound-curing potentiality to the Wf-AgNPs.

Keywords: antioxidant activity; apoptosis; cytotoxicity; silver nanoparticles

INTRODUCTION

Nanotechnology is poised to revolutionize the medical and pharmaceutical industries by introducing a variety of new techniques.[1] Silver nanoparticles (AgNPs), with strong electrical conductivity, act as an antibacterial agent.[2] Exploring the therapeutic properties of AgNPs is crucial as a consequence of their unique characteristics, including high surface area-to-volume ratio, size-dependent physicochemical properties, and inherent antimicrobial activity. These properties make AgNPs promising candidates for various biomedical applications, including antibacterial, anticancer and wound-healing therapies. The silver-coated positively charged plant extract nanoparticle easily binds and penetrates the negatively charged bacterial cell membrane, and inhibits bacterial growth by disrupting the cell membrane and DNA replication by binding with respective enzymes.[3] AgNPs have demonstrated cytotoxic effects against various cancer cell lines by inducing apoptosis, inhibiting cell proliferation and disrupting cancer cell membranes. Their ability to selectively target cancer cells while sparing normal cells makes them promising candidates for cancer therapy.[4] AgNPs exhibit potent wound-healing properties attributed to their antimicrobial activity, promotion of cell

* *Correspondence to: B Chandra Behera, School of Biological Sciences, National Institute of Science Education and Research, Bhubaneswar-752050, Odisha, India. E-mail: bikash@niser.ac.in*

a *Medical Research Laboratory, IMS & SUM Hospital, Siksha 'O' Anusandhan Deemed to be University, Bhubaneswar, India*

b *Department of Biotechnology and Bioinformatics, Sambalpur University, Sambalpur, India*

c *S. K. Dash Center of Excellence of Biosciences and Engineering & Technology, Indian Institute of Technology, Bhubaneswar, India*

d *Department of Food Science Technology and Nutrition, Sambalpur University, Sambalpur, India*

e *School of pharmaceutical sciences, Siksha 'O' Anusandhan Deemed to be University, Bhubaneswar, India*

f *School of Biological Sciences, National Institute of Science Education and Research, Bhubaneswar, India*

proliferation and modulation of inflammatory responses. They can accelerate wound closure, reduce infection rates and improve overall wound-healing outcomes.

In accordance with the current study, *Woodfordia fruticosa*, which contains several potential phytochemicals with potent antimicrobial, antioxidant, anticancer and wound-healing properties characterized by GCMS analysis, was used to create biologically active Ag-NPs using a natural, affordable synthetic method.[5]

Reports on nanoparticles of *W. fruticosa* are scarce, and no report has yet been published on the therapeutic activity of nanoparticles prepared from leaf extract of *W. fruticosa*. Flower extract of silver and gold nanoparticles synthesized from *W. fruticosa* has been studied for antioxidant potential, wound-healing and antibacterial activities.[6,7] As various valuable phytochemicals have already been reported, we hypothesize that the *W. fruticosa* silver nanoparticles (Wf-AgNPs) may have increased therapeutic potential over the typical leaf extract of *W. fruticosa*.

MATERIALS AND METHODS

Collection of *W. fruticosa leaf* and phytochemical extraction

Leaf of *W. fruticose* was collected and identified from the forest area of Gandhmardhan Hills, Western Odisha (20 0 42′– 21 0 00′ N, 82 0 41′–83 0 05′ E) during January 2021. The voucher specimen number of the collected plant is SOA-GDH 013/2021. Collected leaf samples were shade-dried and crushed by a mixer-grinder into powder using a 20-mm mesh to get a uniform size. A 5.0 g sample of the obtained powder was dissolved in 25 mL methanol and placed in the center of a microwave (Ethos Easy advance microwave digestion system; US EPA 3051). The suspension was heated at 70–80°C with a continuous stirring at a specific interval. After heating, the suspension was cooled to room temperature (RT) and centrifuged at 4000 rpm for 5 min. The supernatant was preserved, and the residue obtained was re-extracted using the same solvent and under the same conditions. The supernatant obtained after re-extraction was combined with the earlier one. The dried extract was obtained after being filtered with Whatman No.1 filter paper and evaporating the collected supernatant under reduced pressure.[8]

Preparation of **Wf-AgNPs**

Wf-AgNPs were prepared following the standard method.[9] A solution mixture was made by pouring 10 mL *W. fruticosa* extract with 90 mL of 1 mmol L^{-1} silver nitrate ($AgNO_3$) solution, followed by 30 min mixing at RT. The color change in the mixture revealed the synthesis of Ag nanoparticles. Then the solution was centrifuged at 10000 rpm for 10 min at RT. The AgNPs pellet obtained was washed twice in sterile milliQ water, dried, and then lyophilized for further characterization and analysis.

Characterization of Wf-AgNPs

The prepared Wf-AgNPs were characterized by measuring the absorption spectrum between 300 and 700 nm by a UV-visible spectrophotometer (UV-2600; Shimadzu, Kyoto, Japan) by taking different concentrations (12.5–200 μg mL^{-1}) of Wf-AgNPs solutions. The average size and diameter of the nanoparticles were measured through a particle size analyzer (PSA). The charges and stability of the nanoparticles were obtained through potential Zeta charge (PZC) (Litesizer DLS 500: Anton Paar, Graz, Austria). The surface functional group characteristics of the Wf-AgNPs were detected using a Fourier transform infrared (FTIR) spectroscope (alpha; Bruker, Darmstadt, Germany) by measuring a wave number range from 3500 to 500 cm^{-1}. Further morphological arrangement of the synthesized Wf-AgNPs were confirmed with TEM (F200; JEOL, Tokyo, Japan) operating at 3 kV.

Antioxidant properties

Wf-AgNPs were subjected to 2, 2-diphenyl-1-picrylhydrazyl (DPPH) radical scavenging activity.[10] Ascorbic acid and butylated hydroxytoluene (BHT) were taken as reference standard for the experiment.One milliliter of various extract concentrations (varying from 10 to 100 μg mL^{-1}) was combined with an aliquot of DPPH solution (0.01 mmol L^{-1}), and the final volume was adjusted to 250 μL using methyl alcohol. The solution was mixed and then kept in the dark at RT for 30 min to detect any color change at 517 nm, and the percentage of radical scavenging activity was determined as per the formula below.

$$\text{Percentage of free radical scavenging ability} = CA - SA/CA \times 100 \quad (1)$$

where CA is the control absorbance and SA is thesample absorbance. The gradient of various extract concentrations was considered to estimate the IC50 value.[11]

Assessment of Wf-AgNPs anticancer properties

Human breast cancer cell lines (MCF-7), cervical cancer cell lines (HeLa), human non-small cell lung carcinoma cell line (H1299) and human hepatoma (Hep-G2) cell lines were collected from the National Centre for Cell Science in Pune, India. For anticancer activity detection, these cell lines were exposed to a range of Wf-AgNPs concentrations (12.5–200 μg mL^{-1}) for 72 h before being tested using the sulforhodamine B (SRB) assay at 510 nm to determine the viability of cells. Using an online median inhibitory concentration (IC_{50}) value calculator (AAT Bioquest, Inc., Sunnyvale, CA, USA), the IC_{50} value for the extract was estimated.[12]

Apoptosis assay and DNA fragmentation study

A cell apoptosis experiment was performed by seeding the cells for 24 h, followed by treatment with Wf-AgNPs extract at IC_{50} concentration and incubation for 72 h. After incubation, cells were fixed with 2% formaldehyde, fluorescent stained with 10 μmol L^{-1} DAPI (4′,6-diamidino-2-phenylindole), 10 μmol L^{-1} AO (Acridine orange) and 10 μmol L^{-1} EtBr (Ethidium bromide) for 10 min. Following staining, the cells were washed with 1× phosphate-buffered saline, and fluorescence microscopy (Eclipse Ts2R-FL; Nikon, Tokyo, Japan) was used to take pictures.[12] Furthermore, the above experiment was reconfirmed through the Annexin-V-FITC assay described by Meher *et al.*[13] The TUNEL (Terminal deoxynucleotidyl transferase dUTP nick end labeling) assay was performed to determine whether cells were sensitive to Wf-AgNPs and apoptosis. The Apo BrdU TUNEL test kit from Invitrogen (Carlsbad, CA, USA) was used to examine DNA fragmentation using fluorescence microscopy.[14]

Analysis of mitochondrial membrane potential ($\Delta\Psi m$)

Utilizing JC-1 and DAPI labeling, the effect of Wf-AgNPs on the mitochondrial membrane was assessed utilizing an inverted fluorescent microscope (Eclipse Ts2R-FL; Nikon).[15]

Antibacterial activity of Wf-AgNPs

Four multidrug-resistant (MDR) bacterial strains, *Pseudomonas aeruginosa* (OQ880561), *Acenetobacterbaumannii* (OP889558), *Klebsiella pneumonia* (OQ880560) and *Staphylococcus aureus*

(OQ804432) were collected from different clinical samples from SUM Hospital, Bhubaneswar. The agar well diffusion method was used to determine the Wf-AgNPs antibacterial activity. The standard antibiotic, Linezolid (30 μg mL^{-1}), was used as a control against the Gram-positive bacteria *S. aureus*, whereas Imipenem (10 μg mL^{-1}) was used as a positive control against the Gram-negative bacteria. The micro broth dilution method was used to determine the minimum inhibitory concentration (MIC) and minimum bactericidal concentration (MBC) of the synthesized nanoparticles.[16] SEM was performed to confirm the antimicrobial properties of Wf-AgNPs.[17]

Wound curing activity

The wound-curing property of Wf-AgNPs was determined through excision and incision wound-curing models. An excision wound of 0.2 cm in depth and 2.5 cm in width was generated, which was later infected with multidrug-resistant *S. aureus* strains 50 μL of 1×10^{-8} CFU mL^{-1} in 24 h. During the experiment, four groups of six each animals were formed. Animals in group 1 were used as the negative control (untreated). Animals in group 2 were treated as routine and given Nitrofurazoneointment.Wf-AgNPs were administered to groups 3 and 4 for 14 days from a low dose (50 mg kg body $weight^{-1}$ day^{-1}) to a high dose (100 mg kg body $weight^{-1}$ day^{-1}), respectively. Wound areas were estimated on Day (D)1, D5 and D15, along with the initial wound. All of the experimental methods were authorized by the SOA University of Bhubaneswar's animal Ethics committee (ProtocolIAEC/SPS/SOA/18/2019) with registration number (1171/To/Re/S/)08/TPCSPA.

Detection of phytochemicals

An Exactive Plus Orbitrap high-resolution mass spectrometer connected in tandem with Ultimate 3000 high-performance liquid chromatography (Thermo Fisher Scientific, Waltham, MA, USA) was used to detect the phytochemical compounds present in the plant extract. The intensities of the mass peak and the respective standard curve were compared and annotated through a Python in-house program by parsing it with the PubChem library with a 0.01 m/z error range.

Statistical analysis

Spss v10 for Windows (SPSS, Inc., Chicago, IL, USA) was used for the statistical analysis and a difference with a *P*-value of <0.05 deemed statistically significant.

RESULTS AND DISCUSSION

Preparation and characterization of Wf-AgNPs

The reduction of the Ag ions confirmed the synthesis of Wf-AgNPs. Adding *W. fruticosa* leaf extract at different concentrations (12.5–200 μg mL^{-1}) to aqueous $AgNO_3$ solution changed the solution's colour, confirming the synthesis of Wf-AgNPs.[7] The hue of the solution did not change at 200 μg mL^{-1}, indicating that the synthesis of Wf-AgNPs was saturated. The SPR peaks observed at 450 nm were measured at various Wf-AgNPs concentrations [Fig. 1(A)]. The Highest absorbance was attained at 450 nm at the 200 μg mL^{-1} concentration at RT. This is similar to the findings of Ingarsal *et al*.,[6] who also noticed the maximum absorbance of Wf-AgNPs extracted from flowers at 460 nm. The peak occurring between 420 and 450 nm affirmed the synthesis and existence of Wf-AgNPs owing to its surface plasmon resonance (SPR) character.[18] The functional groups of phytochemicals present in the synthesized Wf-AgNPs are responsible for capping and reducing nanoparticles. These chemical groups were identified via Fourier transform infrared (FTIR) analysis. Several large and small peaks in the range 2942–669 cm^{-1} are depicted in Figure 1(B). The absorption peaks at 2942 cm^{-1} and 2827 cm^{-1} indicated C—H stretching vibrations.[7] The peak at 1717 cm^{-1} and 1650 cm^{-1} indicated the C═O bond of amides. More specifically, the stretching band between 1537 cm^{-1} and 1378 cm^{-1} demonstrated linked vibrations of the carbonyl group (C=O) and the C—H bend of aldehyde groups, respectively.[19] The C—O band of phenolic compounds was attributed to the peak at 1205–1152 cm^{-1}. The peak at 669 cm^{-1} was used to indicate the C—Br band of aliphatic bromo compounds.[20] The tiny peak at 3412 cm^{-1} confirms the O—H stretch of primary aromatic amines or the hydroxyl phenolic (O—H) group. It suggests the binding of Ag^{+} with hydroxyl and/or amine groups of the leaf extract.[6] According to the results of the FTIR analysis, the detected amines, amides, carboxylic, aldehyde, alkane, phenolic and aliphatic bromo compounds are the functional organic molecules that are involved in the synthesis of Wf-AgNPs.[6,19]

High-resolution (HR)TEM was used to further characterize the synthesized Wf-AgNPs with various magnifications (20 nm and 200 nm). According to data obtained, the majority of synthesized particles ranged in size from 20 to 50 nm, with an average particle size of 23 nm, respectively [Fig. 1(C)]. Some of the Wf-AgNPs particles were spherical, prism- and rod-shaped, which corroborated an earlier observation.[7] Additionally, the crystalline character of the Wf-AgNPs, clearly indicated a lattice fringe.

Because it evaluates the hydrodynamic size of the nanoparticles, particle size assessment is more critical in determining particle size. The mean size range of the nanoparticles, determined by the particle size analysis, was 39.63 nm [Fig. 1(D)]. Zeta potential analyses were used to determine the negative charge of the synthesized Wf-AgNPs, which was observed to be −17.0 [Fig. 1(E)]. The synthesized Wf-AgNPs displayed greater stability than those described in a prior study.[21]

Antioxidant properties

Results suggest that the antioxidant activity of Wf-AgNPs elevated along with the concentration and *vice versa* [Fig. **2**(A)]. Lower IC_{50} value signifies higher antioxidant activity. It was observed that the synthesized Wf-AgNPs had remarkably higher antioxidant properties (IC_{50} = 62.28 μg mL^{-1}) compared to the *W ruticosa* leaf extracts (Wf-leaf extracts) (IC_{50} = 69.31 μg mL^{-1}), ascorbic acid (IC_{50} = 75.89 μg mL^{-1}) and BHT (IC_{50} = 87.21 μg mL^{-1}) [Fig. 2(B)]. Phenolic and flavonoid content of Wf-AgNPs was found to be 141.66 ± 8.50 mg GAE/100 g dry weight and 191.66 ± 5.6 mg quercetin equivalent/100 g dry weight. TPC positively correlated with DPPH scavenging activity at the 0.01 level (R^2 = 0.9967) (Fig. 2(C)). TFC and DPPH also positively correlated at 0.01 level (R^2 = 0.9949) (Fig. 2(D)). The observed higher antioxidant properties of Wf-AgNPs than *W. fruticosa* leaf extract, is very similar to the previous report.[22,23] However, the higher antioxidant property of the phyto-nanoparticles than the reference standard Ascorbic acid and agreed with the previous report[10,24] who also observed high antioxidant properties of green synthesized AgNPs compared to standards like ascorbic acid. The higher antioxidant properties of Wf-AgNPs over ascorbic acid and BHT may be due to the presence of secondary metabolites like phenols and flavonoids, which serve as capping agents for the AgNps and can donate hydrogen from their hydroxyl group (-OH) to free radicals and form the stable phenoxyl radicals,[25] Besides, the high

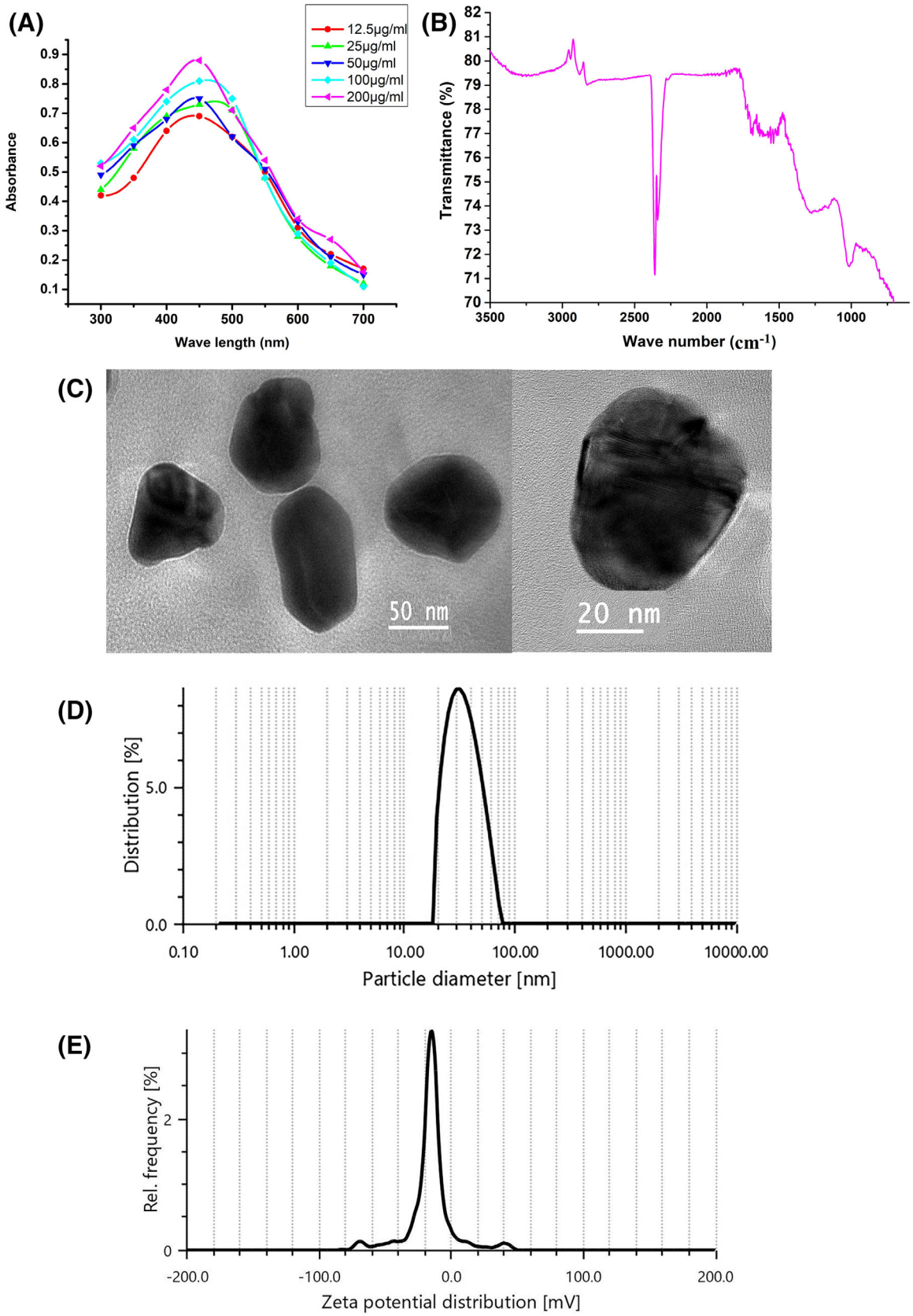

Figure 1. (A) UV-visible spectrum of WfAgNPs from 300 to 700 nm at different concentration. (B) FTIR spectrum of *Wf-* AgNPs. (C) HRTEM images of *Wf*-AgNPs. (D) Particle size analysis of Wf-AgNPs. (E) Zeta potential distribution analysis of Wf-AgNPs

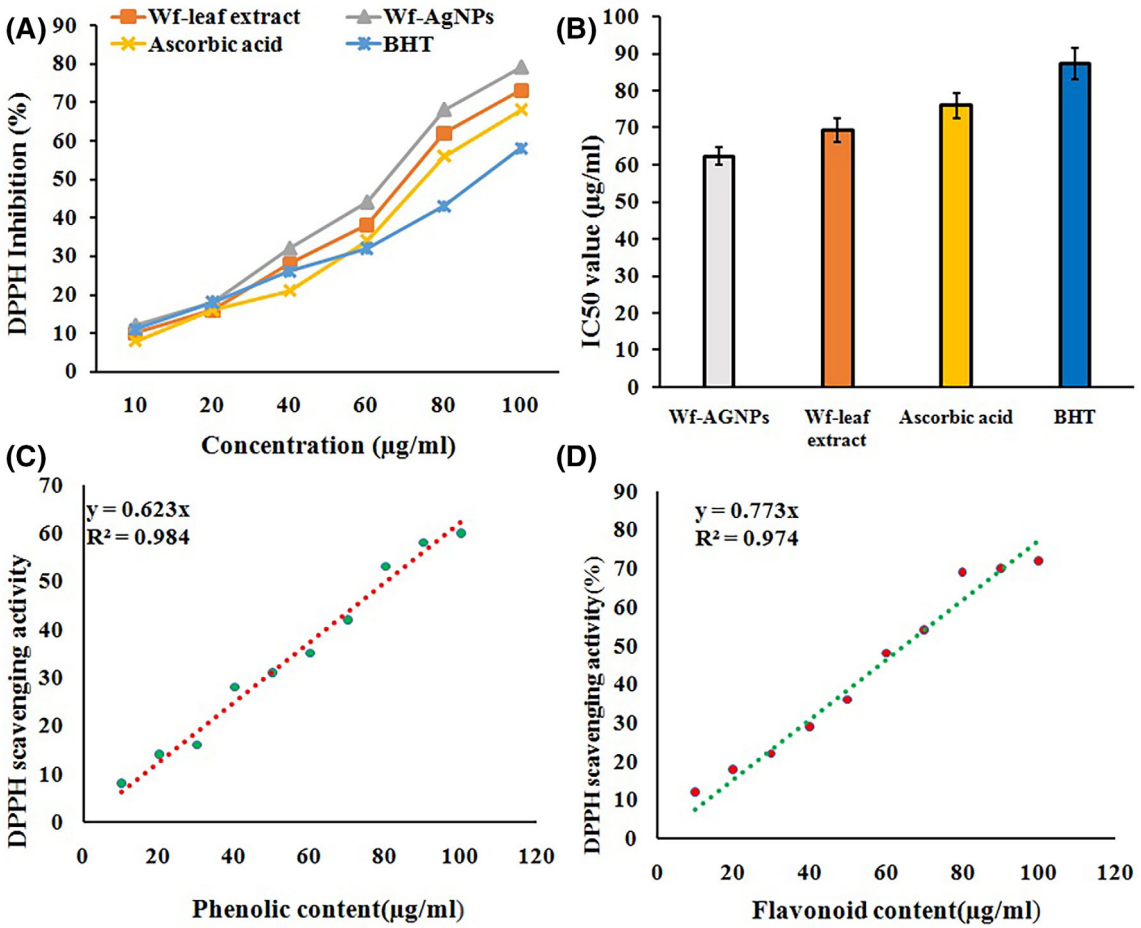

Figure 2. (A) Antioxidant activity and (B) IC 50 value of W. fruticosa, Ascorbic acid and BHT, (C) Corelation between TPC with DPPH scavenging activity, (D) Corelation between TFC with DPPH scavenging activity of Wf-AgNPs.

surface area to volume ratio of the synthesized Wf-AgNPs, may be facilitated the enhanced interaction with reactive oxygen species (ROS) and other oxidative species and their neutralization, subsequently confers the higher antioxidant activity than the traditional antioxidants like ascorbic acid and BHT.[26,27]

Evaluation of anticancer potential

AgNps can slow down the growth of cancer cells by blocking several signaling pathways that are involved in the genesis and progression of tumours.[28] Because of their tendency to interfere with the mitochondrial respiratory chain, which generates reactive oxygen species that can damage DNA, silver nanoparticles are employed as potential cancer therapeutics.[28] Due to their nano size, it can quickly enter through the cancer cell membrane and subsequently into the cancer cell organelles by endocytosis.[29] These accumulated AgNps become cytotoxic to the cancer cell with very little harm to normal cell[s].[29] In the present investigation, the synthesized Wf-AgNPs were treated against various cancer cell lines (MCF-7, HepG2, H1299, Hela). The Wf-AgNPs anticancer activity was evaluated at doses of 12.5 µg/mL to 200 µg/mL (Fig. 3). Cell viability rapidly reduced in a dose-dependent manner as Wf-AgNPs concentration increased (Fig. 3). When Wf-AgNPs were used with various mammalian cell lines, findings of the same kind were also obtained.[30] In the present study, the observed IC 50 values for the respective cell lines are MCF-7(49.2 ± 1.7), HeLa (87.3 ± 1.5), h-1299(104 ± 2.1), and HepG2 (90.4 ± 1.5 µg/mL). In contrast, a significantly lower IC 50 value with AgNPs treated cancer cell lines was observed by Satpathy et al.,[31] The detected cytotoxicity of the treated Wf-AgNPs against tested cell lines may be due to greater cellular uptake and absorption of the treated Wf-AgNPs.[32]

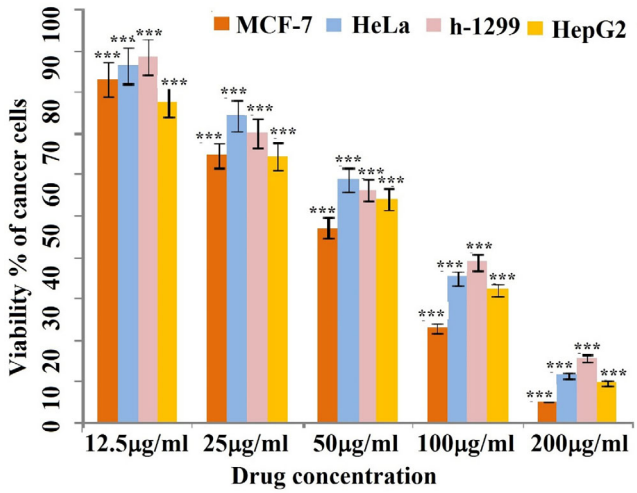

Figure 3. Anticancer activity of Wf-AgNPs tested against different cancer cell lines.

As the MCF-7 cell line exhibits a high induction of cancer cell death with a lower IC50 value (49 µg/mL), it has been the subject of additional investigation.

Apoptosis assay

Apoptosis, or programmed cell death, is regarded as a crucial therapeutic route for the treatment of cancer cells.[29] Apoptotic protein activation, DNA damage, mitochondrial disintegration, and finally, cell shrinkage are the initial steps in the process of apoptosis. These end up being the most crucial targets for cancer treatment.[29] Due to their nano size, AgNps can quickly enter through the cell membrane and induce apoptosis in cancer cells by triggering the synthesis of reactive oxygen species (ROS) by their Ag + ion, which causes cell membrane degradation, oxidative stress, and oxidative damage to cellular contents such as DNA, lipids, and proteins, which may lead to cell death.[29-32] Hence, the apoptosis assay was performed to explore the cell death mechanism in response to the Wf-AgNPs treatment. After being treated with the IC50 concentration of Wf-AgNPs (Fig. 4 (A)), the fraction of early apoptotic and late apoptotic cells against breast cancer cell line (MCF-7) was determined by FACS. Hardly any early apoptotic (5%) and late apoptotic (3%) cells were detected in the control cell lines, possibly due to the typical cell culture damage.

On the other hand, the proportion of early apoptotic cells was substantially higher, 35%, and for late apoptotic, it was 30% in the extract treatment *vs*. the untreated extract ($P < 0.05$). Variations of the viable cell population suggest that Wf-AgNPs-induced anticancer actions cause the cell to undergo apoptosis. Supporting the present finding, a very similar observation was reported by Ullah *et al*.[33] However, a significantly lower percentage of early and late apoptosis was reported by Al-kawmani *et al*.,[34] may be due to variation in the treatment concentration of treatedWf-AgNPs against the MCF-7 cell lines.

Various mechanistic assays, such as the DAPI, Propidium iodide (PI), and Acridine orange (AO), Ethidium Bromide (EB) assays, were employed to investigate and elucidate the mechanism of action of these AgNPs.[33] The use of DAPI, acridine orange, ethidium bromide as well as propidium iodide staining on MCF-7 cancer cells revealed condensed chromatin, membrane blebs, and numerous fragmented nuclei, leading to cell damage and subsequent apoptosis (Fig. 4(B),(D)). A very similar type of membrane and nuclear changes was observed in MCF-7 cells treated with silver nanoparticles synthesized from *Morindapubescens*,[35] *Teucriumstocksianum*.[36]

One key indicator that confirms cells are entering apoptosis is nuclear fragmentation. The TUNEL staining method, which is often referred to as the TUNEL assay, identifies the DNA breaks that arise from DNA fragmentation during the final stages of programmed cell death.[37] The number of TUNEL-positive cells increased progressively after apoptosis was verified and shown in Fig. 4(C). Morphological alterations mimicking apoptosis were most noticeable after Wf-AgNPs treatment. The proportion of TUNEL-positive cells was reduced to control levels after cleavage, suggesting that the extract accelerates DNA degradation in response to cellular stress, leading to apoptotic cell death. This observed outcome is consistent with other studies on the effects of green synthetic nanoparticles on DNA fragmentation.[37]

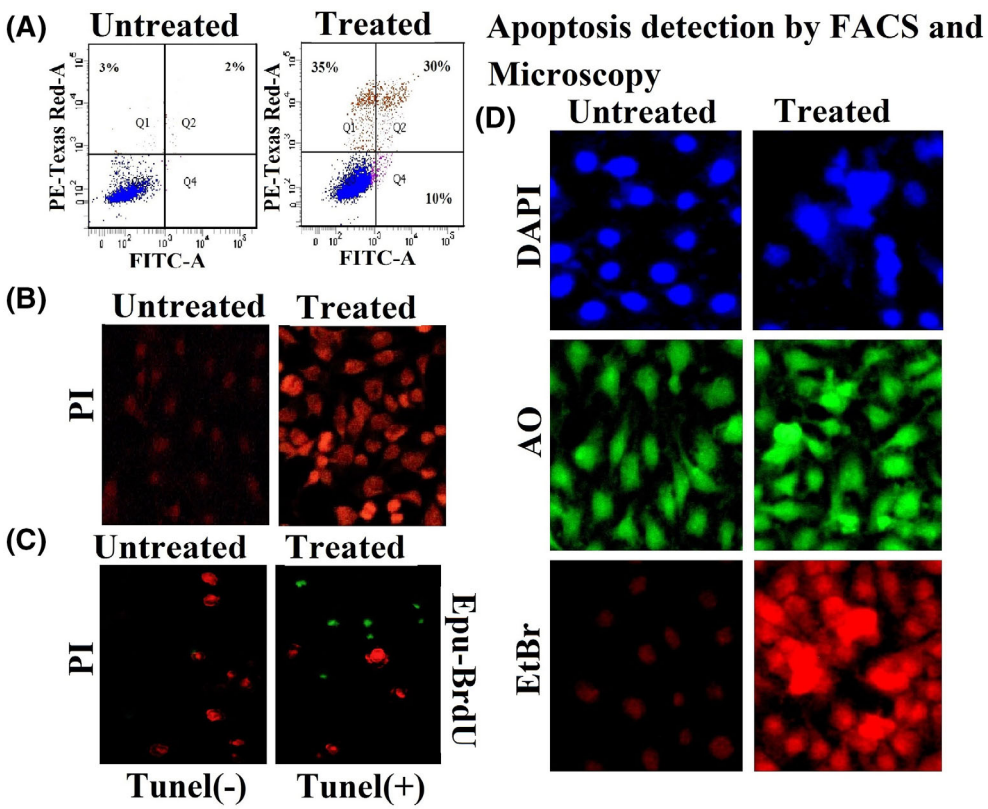

Figure 4. (A) Indicates the FACS study of apoptotic cells against breast cancer cell line (MCF-7), (B) MCF-7 cell line staining with Propidium iodide (D) MCF-7 cell line staining with DAPI, Acridyne Orange and EtBr and (C)TUNEL assay.

Transmembrane potential of mitochondria

Intracellular Ag^{+} released from AgNPs primarily targets mitochondria, the primary ROS source. Dysfunctions such as mitochondrial membrane insufficiency and structural disarray coexist with the stress that AgNPs induce in the mitochondria. Consequently, the cells may die due to cytochrome c being released from the mitochondria and entering the cytoplasm 38. Hence, the toxic effects of AgNPs on mitochondria are analyzed, and it is found that AgNPs' contact interrupts mitochondrial dynamics and biogenesis in MCF-7 cells. The fluorescence intensity of both the untreated and treated MCF7 cells has been measured (Fig. 5). In the case of the JC-1 stain, untreated cells showed mild red fluorescence, whereas treated cells showed robust red fluorescence. Similarly, the rhodamine-123 stain shows bright green in treated cell lines compared to the untreated one. The DAPI stain revealed light blue cells with no morphological changes, whereas the treated cells exhibited brilliant blue cells with morphological changes. All these changes are due to disruption in the transmembrane potential of mitochondria. The present finding is very similar to the previous report of Jain *et al.*,[38] who also observed that the fluorescence-stained biomarkers promote the apoptosis of cells.

Antibacterial assay

The positively charged plant-coated AgNPs have the capability to adhere to the surface of negatively charged bacterial cell membranes, disrupting permeability and respiration processes, which could be the cause of antibacterial activity.[22] The antibacterial activity of Wf-AgNPs was assessed using the agar well diffusion technique on different lawn cultures against four pathogenic MDR bacterial isolates. Their zone of inhibition (ZOI) was in the order of *S. aureus* (32 mm) > *A. baumanii* (26 mm) > *K. pnemoniae* (23 mm) > *P. aeruginosa* (19 mm). The standard antibiotic, Linezolid (30 µg/mL), is used as a positive control against gram-positive *S.aureus*, which showed ZOI 27 mm. In the case of all gram-negative bacteria, imipenem(10 µg/mL) was used, used as a positive control and showed ZOI of 22 mm against *P. aeruginosa*, 26 mm against *K. pneumonia*, and 29 mm against the bacterial strains *A. baumanii*. Similarly, the observed MIC values of the Wf-AgNPs against four selected strains are

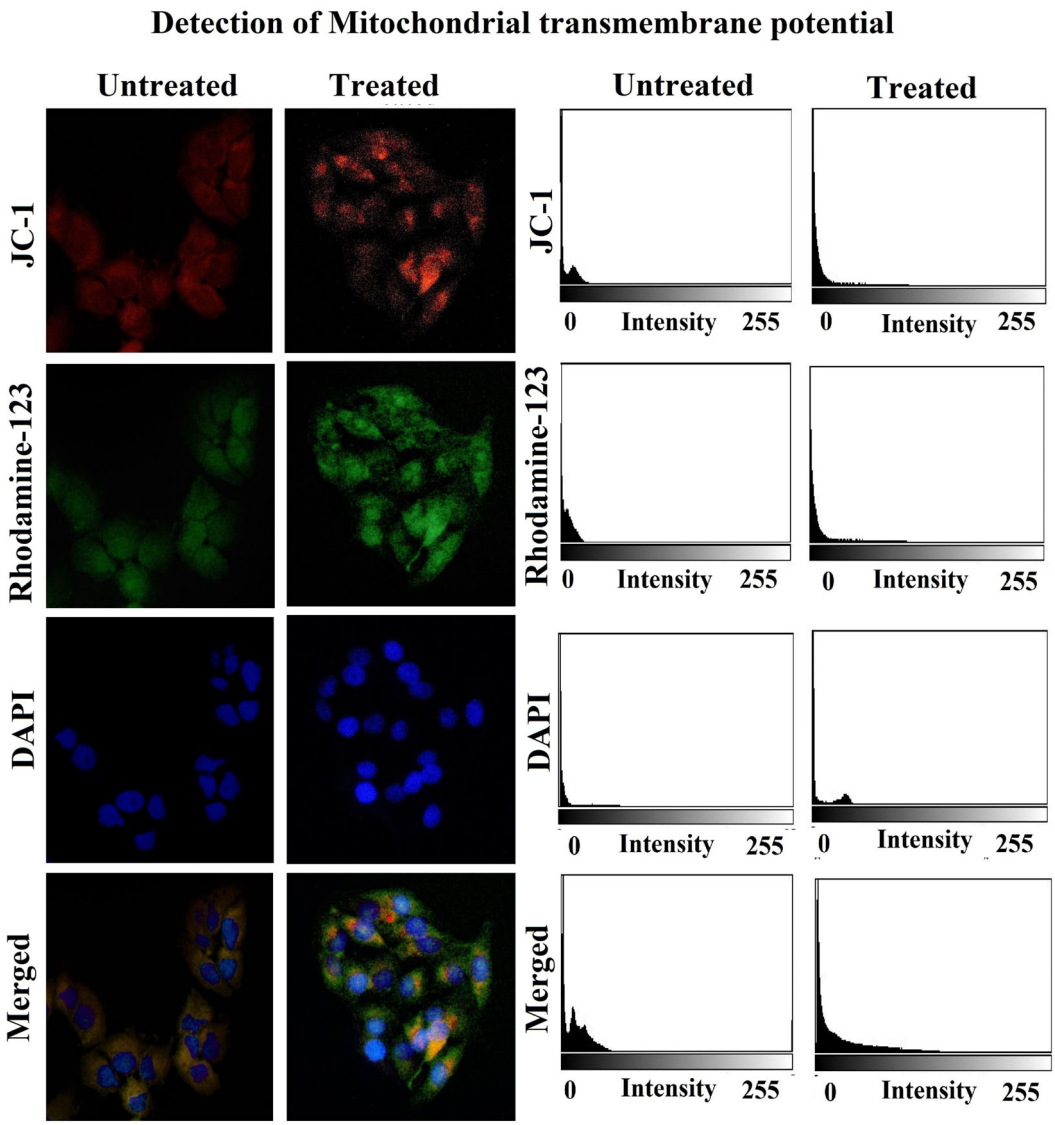

Figure 5. Mitochondrial transmembrane potential study.

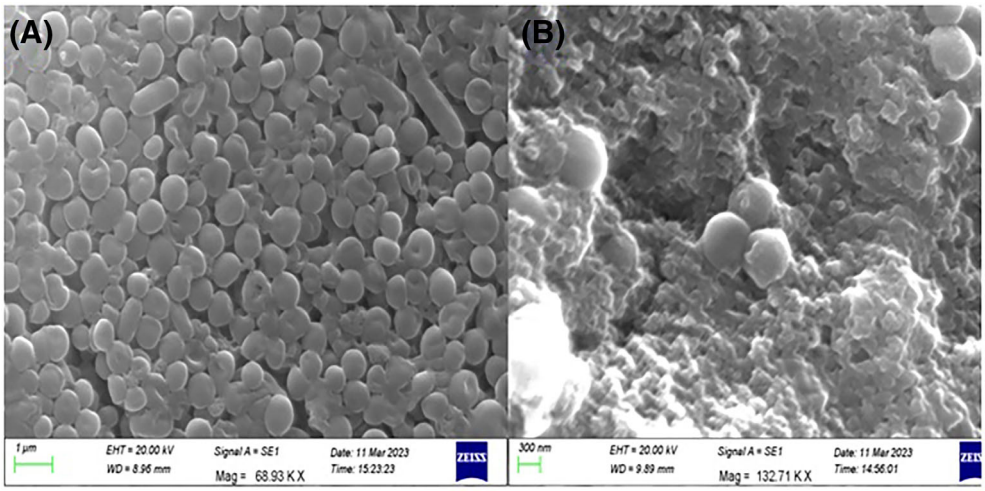

Figure 6. SEM image of (A) untreated and (B) *Wf-AgNPs* treated bacterial strains.

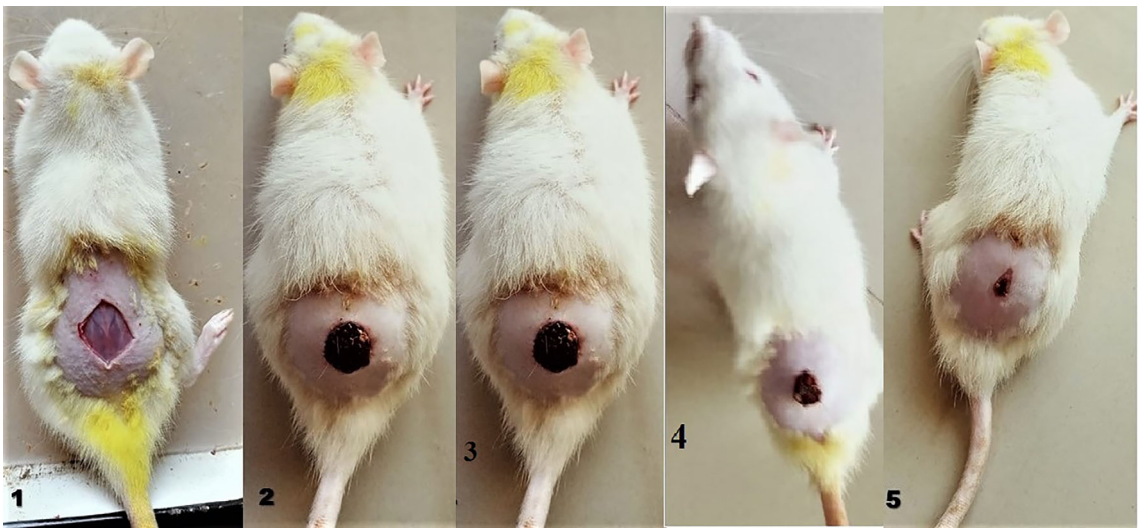

Figure 7. Wound-healing activity of Wf-AgNPs.

S. aureus (0.78 µg/mL), *A. baumanii* (3.12 µg/mL), *K. pneumonia* (1.56 µg/mL), *P. aeruginosa* (3.12 µg/mL). The MBC values detected against *S. aureus, K. pneumoni*a, *A. baumanii*, and *P. aeruginosa* were 3.12, 6.25, 12.5, and 12.5 µg/mL, respectively. The two above standard antibiotics have also been taken as a control to determine MIC value. The binding of silver ions with protein molecules in bacterial cell membranes may be the mechanism through which Wf-AgNPs exert their antibacterial activity, causing damage to the bacterial cell.[39] The results with Wf-AgNPs against the tested bacterial strains were in line with earlier reports of the antibacterial properties of AgNPs made from various plant extracts.[40] The SEM images of the Wf-AgNPs, treated and untreated bacterial cells are depicted in (Fig. 6(A),(B)). It has been observed that the Wf-AgNPs treated bacterial cell showed bacterial cell degradation and lysis compared to the untreated bacterial cell.

Wound healing activity

Excision and incision wound models are commonly used in preclinical studies to evaluate wound healing properties of various pharmaceutical agents.[41] Generally, during excision wound models, a portion of the skin is surgically removed, creating a well-defined wound area. This model allows for the assessment of the size and shape of the wound in terms of contraction, epithelialization, and tissue regeneration, which very closely mimics surgical wounds. However, in incision wound models, a cut was made without removing tissue, and the wound tensile strength and collagen deposition are crucial aspects of wound healing and scar formation.

It has been observed that Wf-AgNPs treatment considerably increased wound-healing activity in both of the examined models compared to the reference standard and control group of animals. **(**Fig. 7). When compared to the control group of animals, those treated with the excision wound model exhibited improved epithelialization rate (10.8 ± 0.67), a significant decrease in wound area ($P < 0.001$), enhanced tissue dry weight ($P < 0.001$) as well as escalating hydroxyproline content ($P < 0.001$) (Table 1).

As depicted in Table 2, compared to the skin-breaking strength of untreated organism (320.2 ± 3.12), the nanoparticle-treated organism showed better skin-breaking strength (410.2 ± 2.36) in

Table 1. Excision wound model of Wf-AgNPs treated and untreated organism

Experimental condition	Untreated control	Standard	Sample (low dose)	Sample (high dose)
Wound area (mm^2) on day 1	185.2 ± 1.12	184.2 ± 0.12	185.2 ± 1.83	186.1 ± 2.65
Wound area (mm^2) on day 5	145.4 ± 0.92	121.4 ± 2.14	132.2 ± 1.12	130.4 ± 2.41
Wound area (mm^2) on day 15	69.2 ± 2.65	38.3 ± 1.52	43.8 ± 1.91**	40.8 ± 1.45**
Period of epithelialization	15.2 ± 0.51	9.9 ± 0.82	11.3 ± 0.42**	10.8 ± 0.67**
Hydroxyproline (mg/kg)	30.4 ± 2.11	56.6 ± 1.33	52.3 ± 2.56**	52.4 ± 1.13**

** $P < 0.01$.

Table 2. Incision wound model of Wf-AgNPs treated and untreated organism

Experimental condition	Untreated control	Standard	Sample (low dose)	Sample (high dose)
Breaking strength (g)	330.2 ± 3.12	476.52 ± 5.12	400.2 ± 4.22**	410.2 ± 2.36
Granulation tissue wet weight (mg)	90.4 ± 3.21	138.4 ± 3.41	118.2 ± 3.2**	120.2 ± 1.3
Granulation tissue wet weight (mg)	15.2 ± 1.23	22.3 ± 0.82	18.8 ± 2.01*	17.3 ± 1.2
Hydroxyproline (mg/kg)	165.7 ± 3.65	225.6 ± 3.53	198.3 ± 2.85	205.3 ± 3.72

*$P < 0.05$;
** $P < 0.01$.

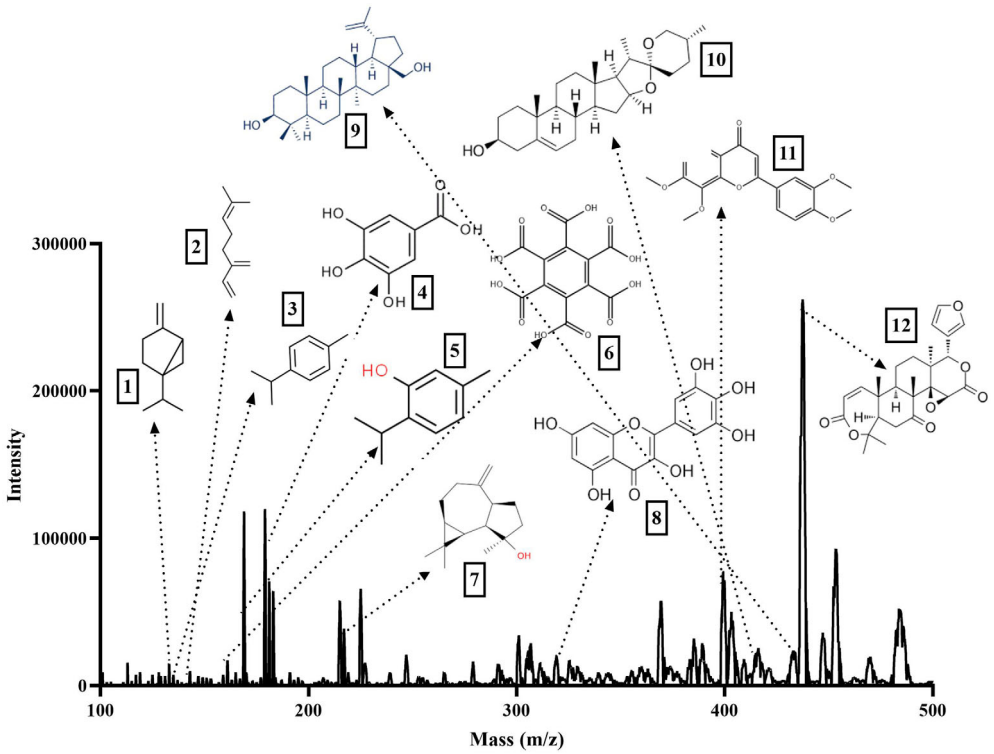

Figure 8. Different antimicrobial compounds present in leaf extract of *Woodfordia fruticosa* (*L.*)

an incision wound model experiment. In comparison to the untreated category of the organism, the Wf-AgNPs treated organism showed the escalated quantity of hydroxyproline amount ($P < 0.001$) and enhanced weight of the granulation tissue ($P < 0.001$), both in lower as well as higher doses of treatment.

A previous study highlighted the wound healing properties of biosynthesis of AgNPs from *Catharanthusroseus* leaf extract using a mice model with effective closure and reducing the size of wounds.[42] Similarly, Lakkim *et al.*[43] explored the wound healing potential of green synthesized AgNPs against MDR bacteria and wound healing efficacy using a murine model by modifying contraction, epithelialization, and tissue regeneration as well as tensile strength and collagen deposition, crucial aspects of wound healing. Supporting the aforementioned result, reports have also

demonstrated how the synthesized Wf-AgNPs, improved re-epithelization and aid in the rapid healing of wounded tissue by raising the tensile strength of the recovered skin tissue comparable to that of healthy skin.[7]

Identification of active phytochemicals by high-Resolution mass spectrometer (**HRMS)**

Plant extracts are the most promising sources of secondary metabolites like protein, phenols, and flavonoids that not only play a role in reducing the respective metal ions into nano size but also play an important role in the capping of nanoparticles. These green synthesized nanoparticles have several therapeutic applications. Though several peaks have been detected through HRMS analysis from the HRMS chromatogram (Fig. 8), 12 major antimicrobial compounds peaks are identified and named as: (i) Sabinene, (ii) Myrcene, (iii) p-cymene, (iv) gallic acid, (v) thymol, (vi) melilotic acid, (vii) spathulenol, (Viii) myricetin, (ix) botulin, (x) diosgenin, (xi) nobiletin, and (xii) obacunone. The identified compounds have already been reported for their anticancer, anti-microbial, anti-viral, antiparasitic, antidiabetic, antitumor, analgesic, local anaesthetic, antinociceptive, cicatrizing properties.[44]

CONCLUSION

For the first time, the leaf extract of *W. fruticosa*, which contains several necessary phytochemicals with potent antimicrobial activity, is used to synthesize silver nanoparticles economically. Characterization of the chemically synthesized nanoparticles revealed the presence of various chemical groups that play an essential role in the synthesis of the nanosphere. HRMS study revealed the presence of multiple phytochemicals containing groups in the synthesized nanoparticles, which confer antimicrobial, antioxidant, anticancer, and wound-curing potential to the Wf-AgNPs. Application of the Wf-AgNPs over the microbial infected wounds showed quick collagen fiber aggregation, generation of new tissue, re-epithelization, and elevation of the tensile strength of the infected skin tissue compared to the standard drugs, leading to rapid wound curing properties of the prepared Wf-AgNPs. Hence, the authors claim an excellent clinical nanoformulation with the *W. fruticosa* leaf extract for the wide therapeutic application.

ACKNOWLEDGEMENTS

We are thankful to the authorities of IMS, and SUM Hospital, Bhubaneswar, for providing research supports.

DATA AVAILABILITY STATEMENT

Data available upon reasonable request from corresponding author.

CONFLICT OF INTEREST

None of the authors have a conflict of interest to disclose.

REFERENCES

1 Mittal J and Jain Rand Sharma MM, Phytofabrication of silver nanoparticles using aqueous leaf extract of *xanthium strumerium L*. and their bactericidal efficacy. *Adv Nat Sci Nanosci Nanotechnol* **8**:025011 (2017).
2 Mohanta YK, Biswas K, Jena SK and Hashem A, Abd_Allah EF, Mohanta TK, anti-biofilm and antibacterial activities of silver nanoparticles synthesized by the reducing activity of phytoconstituents present in the Indian medicinal plants. *Front Microbiol* **11**:1143 (2020).
3 Ameta A, Ameta Rand Ahuja M, photocatalytic degradation of methylene blue over ferric tungstate. *Sci Revs Chem Commun* **3**:172–180 (2013).
4 Sriram MI, Kanth SB, Kalishwaralal K and Gurunathan S, Antitumor activity of silver nanoparticles in Dalton's lymphoma ascites tumor model. *Int J Nanomedicine* **5**:753–762 (2010).
5 Nitha A, Prabha SP, Ansil PN and Latha MS, Antiproliferative effect of Woodfordia fruticosa Kurz flowers on experimentally induced hepato cellular carcinoma in rats and in human hepatoma cell line. *J Pharm Res* **6**:239–248 (2013).
6 Ingarsal N, Kasthuri V, Vinothkanna A and Ananth S, *Woodfordia Fruticosa* flower extract mediated silver nanoparticles and its prodigious potential as antioxidant, antibacterial and photocatalyst. *Ann Rom Soc Cell Biol* **25**:3022–3037 (2021).
7 Raghuwanshi N, Kumari P, Srivastava AK, Vashisth P and Yadav TC, Prasad Rand Pruthi V, synergistic effects of *Woodfordia fruticosa* gold nanoparticles in preventing microbial adhesion and accelerating wound healing in Wistar albino rats in vivo. *Mater Sci Eng C* **80**:252–262 (2017).
8 Li H, Deng Z, Wu T, Liu R, Loewen S and Tsao R, Microwave-assisted extraction of phenolics with maximal antioxidant activities in tomatoes. *Food Chem* **130**:928–936 (2012).
9 Ananth S and Thangamathi P, Larvicidal efficacy of fabricated silver nanoparticles from butea Monosperma flower extract against dengue vector, aedes aegypti. *Biotech Today: Int J Biol Sci* **8**:20–29 (2018).
10 Jena S, Ray A, Banerjee A, Sahoo A, Nasim N, Sahoo S *et al*., Chemical composition and antioxidant activity of essential oil from leaves and rhizomes of Curcuma angustifolia Roxb. *Nat Prod Res* **31**:2188–2191 (2017).
11 Ghosh S, Derle A, Ahire M, More P, Jagtap S, Phadatare SD *et al*., Phytochemical analysis and free radical scavenging activity of medicinal plants *Gnidiaglauca* and *Dioscorea bulbifera*. *PLoS One* **8**:82529 (2013).
12 Behera S, Monalisa K, Meher RK, Mohapatra S, Madkami SK, Das PK *et al*., Phytochemical fidelity and therapeutic activity of micropropagated Curcuma amada Roxb.: a valuable medicinal herb. *Ind Crop Prod* **176**:114401 (2022).
13 Meher RK, Pragyandipta P, Reddy PK, Pedaparti R, Kantevari S and Naik PK, Development of 1, 3-diynyl derivatives of noscapine as potent tubulin binding anticancer agents for the management of breast cancer. *J Biomol Struct Dyn* **40**:13136–13153 (2022).
14 Crowley LC, Marfell BJ and Waterhouse NJ, Detection of DNA fragmentation in apoptotic cells by TUNEL. *Cold Spring Harb Protoc* **10**:pdb-prot087221 (2016).
15 Rovini A, Heslop K, Hunt EG, Morris ME, Fang D, Gooz M *et al*., Quantitative analysis of mitochondrial membrane potential heterogeneity in unsynchronized and synchronized cancer cells. *FASEB J* **35**:e21148 (2021).
16 Dubey D, Sahu MC, Rath S, Paty BM, Debata NK and Padhy RN, Antimicrobial activity of medicinal plants used by aborigines of Kalahandi, Orissa, India against multidrug resistant bacteria. *Asian Pac J Trop Biomed* **2**:S846–S854 (2012).
17 Singh PandMijakovic I, Antibacterial effect of silver nanoparticles is stronger if the production host and the targeted pathogen are closely related. *Biomedicine* **10**:628 (2022).
18 Mohanta YK, Panda SK, Biswas K, Tamang A, Bandyopadhyay J, De D *et al*., Biogenic synthesis of silver nanoparticles from Cassia fistula (Linn.): in vitro assessment of their antioxidant, antimicrobial and cytotoxic activities. *IET Nanobiotechnol* **10**:438–444 (2016).
19 Hajebi S, Tabrizi MH and Moghaddam MN, Shahraki Fand Yadamani S, rapeseed flower pollen bio-green synthesized silver nanoparticles: a promising antioxidant, anticancer and antiangiogenic compound. *J Biol Inorg Chem* **24**:395–404 (2019).
20 Mohanta YK, Mishra AK, Nayak D, Patra B, Bratovcic A, Avula SK *et al*., Exploring dose-dependent cytotoxicity profile of Gracilaria edulis-mediated green synthesized silver nanoparticles against MDA-MB-231 breast carcinoma. *Oxidative Med Cell Longev* **2022**:15 (2022). https://doi.org/10.1155/2022/3863138.
21 Maniknandan DB, Sridhar A, Sekar RK, Perumalsamy B, Veeran S, Arumugam M *et al*., Fabrication, characterization of silver nanoparticles using aqueous leaf extract of Ocimum Americanum (hoary basil)

and investigation of its in vitro antibacterial, antioxidant, anticancer and photolytic reduction. *J Environ Chem Eng* **9**:104845 (2021).
22 Salari S, Bahabadi SE, Samzadeh-Kermani A and Yosefzaei F, *In-vitro* evaluation of ntioxidant and antibacterial potential of green synthesized silver nanoparticles using *Prosopis farcta* fruit extract. *Iran J Pharm Res* **18**:430–445 (2019).
23 Mohanta YK, Panda SK, Jayabalan R, Sharma N, Bastia AK and Mohanta TK, Antimicrobial, antioxidant and cytotoxic activity of silver nanoparticles synthesized by leaf extract of Erythrina suberosa (Roxb.). *Front Mol Biosci* **4**:14 (2017).
24 Patra JK and Baek KH, Green synthesis of silver chloride nanoparticles using *Prunuspersica L*. outer peel extract and investigation of antibacterial, anticandidal, antioxidant potential. *Green Chem Lett Rev* **9**:132–142 (2016).
25 Yousaf H, Mehmood H, Ahmad KS and Raffi M, Green synthesis of silver nanoparticles and their applications as an alternative antibacterial and antioxidant agents. *Mater Sci Eng C Mater Biol Appl* **112**: 110901 (2020).
26 Essghaier B, Dridi R, Mottola F, Rocco L, Zid MF and Hannachi H, Biosynthesis and characterization of silver nanoparticles from the extremophile plant Aeonium haworthii and their antioxidant, antimicrobial and anti-diabetic capacities. *Nanomaterial* **13**:100 (2023).
27 El-Ansary AE, Omran AAA, Mohamed HI and El-Mahdy OM, Green synthesized silver nanoparticles mediated by *fusarium nygamai* isolate AJTYC1: characterizations, antioxidant, antimicrobial, anticancer, and photocatalytic activities and cytogenetic effects. *Environ Sci Pollut Res* **30**:100477–100499 (2023).
28 Felimban AI, Alharbi NS and Alsubhi NS, Optimization, characterization, and anticancer potential of silver nanoparticles biosynthesized using *Olea europaea*. *Int J Biomater* **2022**:12 (2022).
29 Al-Zahrani SA, Bhat RS, Al-Onazi MA, Alwhibi MS, Soliman DA, Aljebrin NA *et al*., Anticancer potential of biogenic silver nanoparticles using the stem extract of Commiphora gileadensis against human colon cancer cells. *Green Process Synth* **11**:435–444 (2022).
30 Sambale F, Wagner S, Stahl F, Khaydarov RR, Scheper T and Bahnemann D, Investigations of the toxic effect of silver nanoparticles on mammalian cell lines. *J Nanomater* **2015**:136765 (2015).
31 Satpathy S, Patra A, Ahirwar B and Hussain MD, Antioxidant and anticancer activities of green synthesized silver nanoparticles using aqueous extract of tubers of *Puerariatuberosa*, artificial cells. *Nanomed Biotechnol* **46**:S71–S85 (2018).
32 Wei Z, Hao J, Yuan S, Li Y, Juan W, Sha X *et al*., Paclitaxel-loaded Pluronic P123/F127 mixed polymeric micelles: formulation, optimization and in vitro characterization. *Int J Pharm* **376**:176–185 (2009).
33 Ullah I, Khalil AT, Ali M, Iqbal J, Ali W, Alarifi S *et al*., Green-synthesized silver nanoparticles induced apoptotic cell death in MCF-7 breast cancer cells by generating reactive oxygen species and activating caspase 3 and 9 enzyme activities. *Oxidative Med Cell Longev* **2020**: 1215395 (2020).
34 Al-kawmani AA, Alanazi KM, Farah MA, Ali MA, Hailan WAQ and Al-Hemaid FM, Apoptosis-inducing potential of biosynthesized silver nanoparticles in breast cancer cells. *J King Saud Univ Sci* **32**:2480–2488 (2020).
35 Inbathamizh L and PonnuTM MEJ, In vitro evaluation of antioxidant and anticancer potential of Morindapubescens synthesized silver nanoparticles. *J Pharm Res* **6**:32–38 (2013).
36 Ullah I, Abamor EŞ, Bağirova M, Shinwari ZK and Allahverdiyev AM, Biomimetic production, characterisation, in vitro cytotoxic and anticancer assessment of aqueous extract-mediated AgNPs of TeucriumstocksianumBoiss. *IET Nanobiotechnol* **12**:270–276 (2018).
37 Zhang K, Liu X, Ravi SOAS, Ramachandran A, Ibrahim IAA, Nassir AM *et al*., Synthesis of silver nanoparticles (AgNPs) from leaf extract of *salvia miltiorrhiza* and its anticancer potential in human prostate cancer LNCaP cell lines. *Artif Cells Nanomed Biotechnol* **47**:2846–2854 (2019).
38 Jain N, Jain P, Rajput D and Patil UK, Green synthesized plant-based silver nanoparticles: therapeutic prospective for anticancer and antiviral activity. *Micro Nano Syst Lett* **9**:5 (2021).
39 Lok CN, Ho CM, Chen R, He QY, Yu WY, Sun H *et al*., Proteomic analysis of the mode of antibacterial action of silver nanoparticles. *J Proteome Res* **5**:916–924 (2006).
40 Mohanta YK and Behera SK, Biosynthesis, characterization and antimicrobial activity of silver nanoparticles by Streptomyces sp. SS2. *Bioprocess Biosyst Eng* **37**:2263–2269 (2014).
41 Wilhelm KP, Wilhelm D and Bielfeldt S, Models of wound healing: an emphasis on clinical studies. *Skin Res Technol* **23**:3–12 (2017).
42 Al-Shmgani HSA, Mohammed WH, Sulaiman GM and Saadoon AH, Biosynthesis of silver nanoparticles from Catharanthus roseus leaf extract and assessing their antioxidant, antimicrobial, and wound-healing activities. *Artif Cell Nanomed Biotechnol* **45**:1–7 (2017).
43 Lakkim V, Reddy MC, Pallavali RR, Reddy KR, Reddy CV, Inamuddin BAL *et al*., Green synthesis of silver nanoparticles and evaluation of their antibacterial activity against multidrug-resistant bacteria and wound healing efficacy using a murine model. *Antibiotics* **9**:902 (2020).
44 Das PK, Goswami S, Chinniah A, Panda N, Banerjee S, Sahu NP *et al*., *Woodfordia fruticosa*: traditional uses and recent findings. *J Ethnopharmacol* **110**:189–199 (2007).